Materials Science Forum Vol. 352 (2000) pp. 49-56
online at http://www.scientific.net

Electrodeposition of Cu-Al Alloys and Underpotential Deposition of Al onto Cu Single Crystals from a Room-Temperature Chloroaluminate Molten Salt

G.R. Stafford[1], V.D. Jović[1] and C.L. Hussey[2]

[1] Materials Science and Engineering Laboratory, National Institute of Standards and Technology, Gaithersburg, MD 20899-8551, USA

[2] Department of Chemistry, University of Mississippi, Mississippi, MS 38677, USA

Keywords: Cu(100), Cu(110), Cu(111), Cu-Al Alloys, Electrodeposition, Phase Composition, Room-Temperature Molten Salt, UPD of Al

onto Cu(111), Cu($1\bar{0}0$) and Cu(110) faces, were investigated in the Lewis acidic aluminum chloride/1-methyl-3-ethyl-imidazolium chloride. It was shown that it is possible to produce Cu-Al alloy deposits at potentials positive of that corresponding to the electrodeposition of bulk Al (≈0 V). For a 0.05 mol dm^{-3} solution of Cu(I), the onset of the Al codeposition process was found to occur at around 0.30 V versus the Al(III)/Al couple; however, a limiting current for the reduction of Cu(I) to pure Cu metal can be observed in the 0.60 V to 0.30 V potential interval in this solution. The Cu-Al alloy composition was found to be independent of the Cu(I) concentration, reaching a maximum value of 43 atomic percent (a/o) Al at 0 V. X-ray diffraction studies indicated that Cu-Al deposits containing about 7.2 a/o Al retained the fcc Cu structure; however, deposits containing 12.8 a/o Al were two-phase with the second phase tentatively identified as martensitic ß'-Cu_3Al. This phase appears to form before fcc Cu becomes saturated with Al. Cyclic voltammograms recorded onto Cu(111), Cu(100) and Cu(110) clearly indicate that UPD of Al commences at about 0.3 V vs. Al. On the (111) face of Cu UPD takes place through two sharp and separated peaks, indicating formation of two different adsorbed structures, with the second peak corresponding to the formation of a monolayer of Al. Surface alloying of Cu with Al was detected at potentials of the first peak (≈ 0.25 V vs. Al).

1. INTRODUCTION

Several molten salt systems have been investigated for the electrodeposition of Al and its alloys. One of the more popular of these systems is a mixture of AlX_3 (X = Br or Cl) with either alkali metal or organic halide salts. Binary mixtures of $AlCl_3$ and alkali metal chlorides are molten at temperatures as low as 108 °C. Systems which are molten at room temperature can be obtained when the alkali chloride is replaced with certain unsymmetrical quaternary ammonium chloride salts such as 1-methyl-3-ethylimidazolium chloride (MeEtimCl) [1].

In the equimolar mixture of $AlCl_3$ and MeEtimCl melts, an ionic liquid composed exclusively of $MeEtim^+$ and $AlCl_4^-$ is produced. When the relative concentrations deviate from equimolar, additional ionic species are introduced. Cl^- is present in melts containing excess MeEtimCl while higher order Al complexes, such as $Al_2Cl_7^-$, are present with excess $AlCl_3$. The chemical equilibria operative in $AlCl_3$-MeEtimCl melts under a wide range of $AlCl_3$ concentrations above the equimolar point are well known [2]. This melt is often considered as an acid-base system described by the reaction:

$$2AlCl_4^- \Leftrightarrow Al_2Cl_7^- + Cl^- \quad (1)$$

The equilibrium constant for Eq. 1 is reported to be 5.0×10^{-17} at 40 °C [2]. Aluminum can be electrodeposited only by the reduction of the $Al_2Cl_7^-$ complex since $MeEtim^+$ is reductively decomposed at potentials positive of $AlCl_4^-$ reduction. The Al deposition reaction, involving $Al_2Cl_7^-$ as the electroactive species, is normally expressed by Eq. 2.

$$4Al_2Cl_7^- + 3e \Rightarrow Al + 7AlCl_4^- \quad (2)$$

Aluminum alloys can be electrodeposited from chloroaluminate electrolytes with the addition of the solute metal ion to the electrolyte. This can be accomplished by either anodic dissolution of the solute metal directly into the melt or by the addition of the appropriate chloride salt. The formation of Al-transition metal alloys is also possible even though the deposition potential of the transition metal may be several hundred millivolts more positive than that of Al. The mechanism leading to the formation of these alloys involves the underpotential deposition (UPD) of Al during the mass-transport-limited electrodeposition of the transition metal. Such interesting alloy formation has been demonstrated for Al-Ni [3] from $AlCl_3$:NaCl electrolyte as well as Al-Ni [4-6], Al-Co [7,8] and Al-Cu [9,10] from the room temperature chloroaluminates. In this article, we describe the electrodeposition of Cu and the underpotential co-deposition of Al with Cu to form Cu-Al alloys from solutions of Cu(I) in the Lewis acidic $AlCl_3$-MeEtimCl melt. In addition we will describe the UPD of Al onto Cu(111), Cu(110), Cu(100) single crystal surfaces.

2. EXPERIMENTAL

The nitrogen-filled glove box system and the method used to evaluate the quality of the glove box atmosphere have been described [11]. The electrochemical instrumentation and the electrochemical cell with reference and counter electrodes were identical to those employed during a previous investigation [8]. Experiments of Cu-Al alloy electrodeposition were conducted in the 60:40 mole ratio $AlCl_3$: MeEtimCl melt at (40±1)°C. All potentials are referenced to the Al(III)/Al couple in this melt.

MeEtimCl was synthesized from ethyl chloride and 1-methylimidazole (Aldrich, 99%)* and recrystallized from acetonitrile-ethyl acetate mixtures as described in the literature [12]. All traces of protonic impurities were removed from the melt by pre-electrolyzing the melt between Al electrodes (Alfa/ESAR, puratronic, 99.999%) for several days while the melt was stirred. The melt was filtered through a medium porosity glass frit to remove any Al debris that may have detached from the cathode during the electrolysis step, and it was then evacuated to 1.3×10^{-3} Pa for 24 h.

Cu single crystals (Monocrystals Comp.) were mechanically polished on fine grade emery papers (1200, 2400 and 4000) with subsequent polishing on polishing clothes impregnated with ssuspension of polishing alumina with particle dimensions of 1 μm, 0.3 μm and 0.05 μm. After chemical polishing Cu single crystals were electrochemically polished in a solution of 85 % phosphoric acid at a constant voltage of 1.7 V (vs. Pt counter electrode) until the current density droped to a value of about 18 mA cm^{-2}. Electrodes were then thoroughly washed with pure water (Barnstead - EASY pure UV). Water was removed from the electrode surfaces by the stream of nitrogen and electrodes were transferred into the glove box.

---

* Certain commercial materials and instruments are identified in this report to adequately specify the experimental procedure. In no instance does such identification imply recommendation or endorsement by the National Institute of Standards and Technology, nor does it imply that the material identified is necessarily the best available for this purpose.

Bulk alloy deposits were characterized with scanning electron microscopy (SEM), energy dispersive x-ray spectrometry (EDS), and x-ray diffraction (XRD). The x-ray diffraction patterns were collected on a Scintag diffractometer using Cu-K_α radiation and a Ge solid state detector. Lattice parameters were determined by least squares refinement, using the reflections from the nickel substrate as an internal standard.

3. RESULTS AND DISCUSSION

3.1. Electrodeposition of Cu-Al alloys

Cu(I) was introduced into the melt by the electrodissolution of a Cu wire anode at a potential of 0.85 V. The weight loss of the Cu anode was determined after the passage of a given charge, and calculations based on these measurements confirmed that Cu(I) was the anodization product.

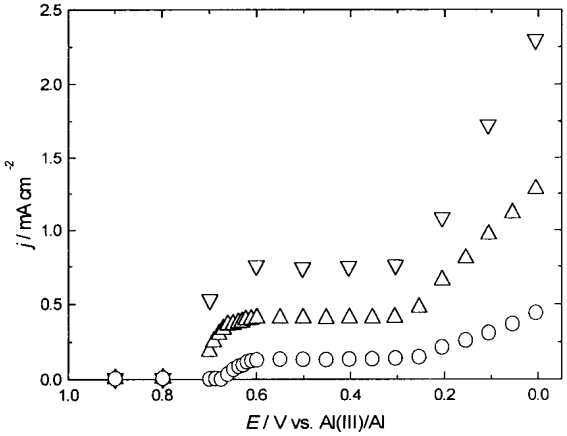

Fig. 1. Current-sampled voltammograms recorded at a stationary Pt electrode in solutions of Cu(I) in the 60.0-40.0 m/o melt at 40±1 °C. The Cu(I) concen-trations were: (○) 0.010 mol dm^{-3}; (△) 0.025 mol dm^{-3}; and (▽) 0.050 mol dm^{-3}. The current was sampled at 10 s following the application of each potential pulse.

Fig. 1 shows a series of sampled-current or pulse voltammograms constructed from chronoamperometric current-time transients that were recorded at a platinum disk electrode in unstirred 0.010, 0.025, and 0.050 mol dm^{-3} solutions of Cu(I) in the 60.0-40.0 m/o melt. The data used to construct these voltammograms were obtained by stepping the electrode potential from an initial value of 1.50 V, where no Faradaic reaction takes place, to the potential of interest. The current was sampled at 10 s following the application of the potential pulse. The resulting electrodeposit was then stripped from the electrode by holding the potential at 1.50 V for 30 s while the solution was stirred, and then the entire process was repeated at another potential. All three voltammograms exhibit well-defined limiting currents due to the mass-transport-controlled deposition of Cu. In addition, these voltammograms show a rise in current beginning at about 0.25 V, which is due to the co-deposition of Al with Cu to produce a Cu-Al alloy, $Cu_x Al_{1-x}$, where $1 > x > 0$. The overall deposition reaction is shown in Eq. 3

$$xCu^{+}(solv) + 4(1 - x)Al_2Cl_7^{-} + (3 - 2x)e^{-} \Leftrightarrow Cu_x Al_{1-x} + 7(1 - x)AlCl_4^{-} \qquad (3)$$

The limiting currents of the voltammograms in Fig. 1 were found to vary linearly with the Cu(I) concentration. The diffusion coefficient of Cu(I), $D_{Cu(I)}$, was calculated from these limiting currents by using the Cottrell equation. The average value of $D_{Cu(I)}$ is $(3.6 \pm 0.5) \times 10^{-7}$ cm^2 s^{-1}, and the Stokes-Einstein product, $D_{Cu(I)}\,\eta/T$, where η and T are the absolute viscosity and tempera-ture, respectively, is 1.9×10^{-10} g cm s^{-2} K^{-1}.

The Cu-Al alloy compo-sition, represented for conve-nience as the fraction of Al in the alloy, 1 - x, was estimated from the voltammograms in Fig. 1 by using the following expression

$$1 - x = 1/\{1 + 3[j_L/(j_t - j_L)]\} \quad (4)$$

where j_L is the limiting current for the copper deposition reaction depicted in Fig. 1, and j_t is the total current observed at potentials where the co-deposition of Al is observed. Plots of 1 - x versus E based on these calculations are given in Fig. 2 for three different Cu(I) concentrations. Examination of the data in this plot reveals that the Cu-Al alloy composition is independent of the Cu(I) concentration over the range of concentrations that were examined in this study.

Taken together, the results presented above suggest that at a fixed potential the rate of alloy formation is determined by the mass-transport-limited reduction of Cu(I) and, as a result, the rate of alloy formation increases in direct proportion to an increase in the Cu(I) concentration. Thus, under the conditions of the present study, the concentration of $Al_2Cl_7^-$ does not play a role in determining the rate of alloy formation because the concentration of this ion is in large excess (1.95 mol dm^{-3}) over the Cu(I) concentration, i.e., the reaction depicted in Eq. 3 can be considered to be pseudo-first order in Cu(I). Somewhat different results were found during previous investigations involving the UPD of Co-Al [8] and Ni-Al [6] in acidic $AlCl_3$-MeEtimCl. At a fixed potential, the compositions of these alloys varied with the concentrations of the respective transition metal ions in the deposition solution, even though the transition metal ions were undergoing reduction at the mass transport limited rate during alloy formation. This suggests that in both cases the Al co-deposition process is kinetically hindered.

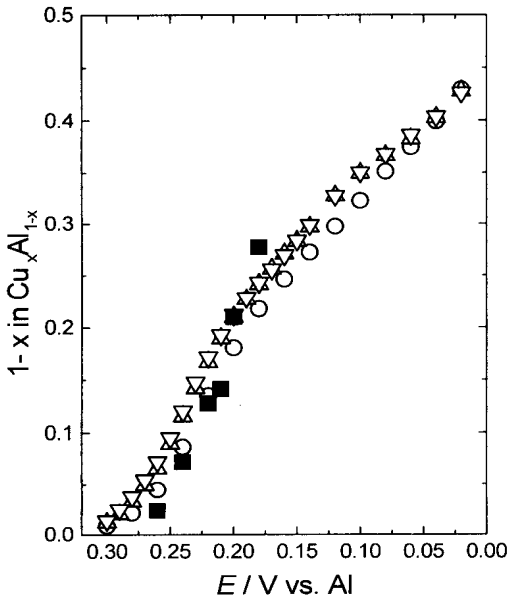

Fig. 2. Fraction of Al in Cu-Al alloy, 1 - x, as a function of potential from Fig. 1:
(○) 0.010 mol dm^{-3} Cu(I);
(△) 0.025 mol dm^{-3} Cu(I); and
(▽) 0.050 mol dm^{-3} Cu(I);
(■) AAS analysis of bulk electrodeposits.

Several bulk electrodeposits were prepared on 0.10 cm nickel wire at potentials ranging from 0.40 V to 0 V at 25°C from 60-40 m/o melt containing 0.10 mol dm^{-3} Cu(I) at 25 °C. Based on the charge passed, the nominal thickness of these deposits ranged from 10 to 15 μm. The compositions of some of these deposits were determined by atomic absorption spectrophotometry (AAS) after the deposits were dissolved from the substrates with 1:1 HNO_3-HCl. Prior to dissolution, the deposits were examined by EDS to ensure that no chloride was present. Within the detection limits of EDS, all of the deposits were found to be either pure Cu or Cu-Al alloy. The AAS results, which are shown in Fig. 2, are in excellent agreement with the alloy compositions determined by sampled current voltammetry.

The x-ray diffraction patterns from several electrodeposits are shown in Fig. 3. In all cases, reflections from the nickel substrate (see figure caption) are clearly visible and increase in intensity as the deposition potential becomes more negative. This is a clear indication that the total mass of the deposit is reduced, either by Al incorporation or because of reduced thickness. Deposits formed at potentials between 0.30 V and 0.40 V exhibit diffraction patterns that are consistent with pure Cu. The deposit formed at 0.24 V, which

contains 7.2 a/o Al, retains the face-centered cubic (fcc) structure. The reflections are shifted to slightly lower values of 2θ, indicating that the lattice is expanding as Al alloys substitutionally with Cu [13]. The reflections broaden somewhat, indicating a reduced grain size or the presence of nonuniform strain. The maximum solubility of Al into fcc Cu under equilibrium conditions is reported to be 19.7 a/o [13].

Several changes in the crystal structure are seen in the 0.22 V electrodeposit, which contains 12.77 a/o Al. The first is the continued expansion of the fcc Cu lattice and reflection broadening. The second is the appearance of a second phase, which we have tentatively identified as martensitic Cu_3Al (β'). It is well known that in the Cu-Al system, β' martensite is formed upon cooling from the high temperature variant β-Cu_3Al, which has a body-centered (bcc) structure [14]. There is also precedence for its electrodeposition from a nonaqueous ethylbenzene-toluene solution [15]. The crystal structure of the β' phase can be described by a disordered, orthorhombic lattice having lattice constants of a = 0.449 nm, b = 0.519 nm, and c = 3.82 nm and consisting of a stacking sequence of 18 close-packed layers [14]. Deposits prepared at 0.22 V and 0.21 V clearly show the (202) and (12 $\underline{10}$) reflections for the β' phase. It is not until the deposition potential is reduced to 0.20 V, where the Al composition reaches 21.0 a/o, that the (00$\underline{18}$) β' reflection can be resolved from the Cu(111). The lattice parameters calculated from the three β'-Cu_3Al reflections from this deposit were a = 0.449 nm, b = 0.537 nm, and c = 3.834 nm, with an uncertainty of 0.12 %. Alloys electrodeposited at 0.10 V and 0.0 V showed reflections for the nickel substrate alone. This may be the result of poor deposit morphology and the subsequent loss of material through handling, or it may be an indication that the deposit is simply amorphous.

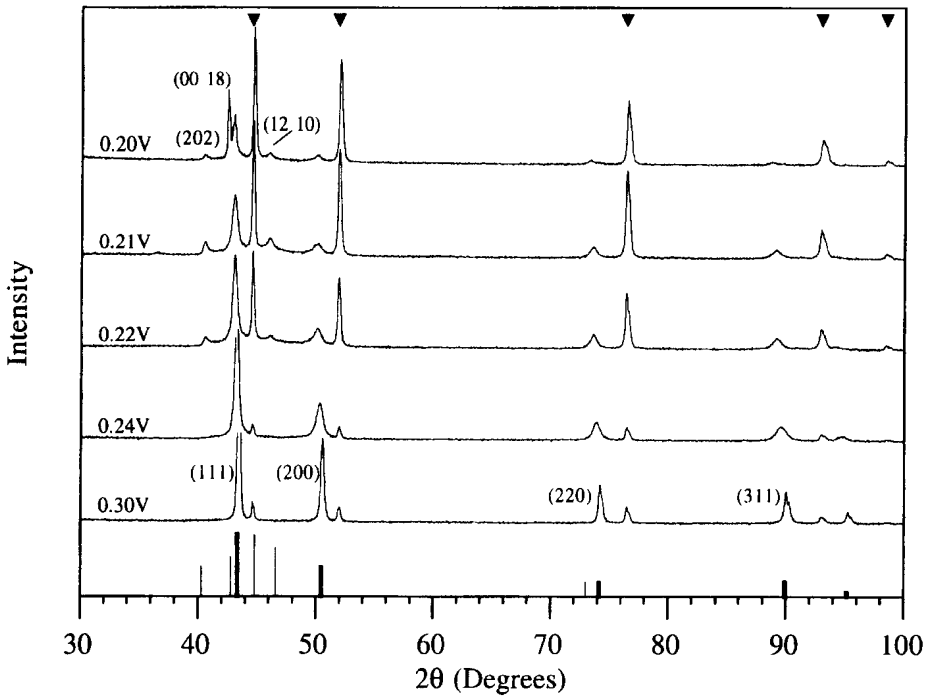

Fig. 3. XRD patterns (Cu-Kα) of Cu-Al alloys electrodeposited at different potentials marked in the figure. The bold vertical lines represent the reflections for Cu, JCPDS card# 4-0836, and the thin vertical lines represent the reflections for orthorhombic Cu_3Al, JCPDS card# 28-0005. The triangles represent reflections originating from the nickel substrate.

3.2. UPD of Al onto Cu(111), Cu(100) and Cu(110)

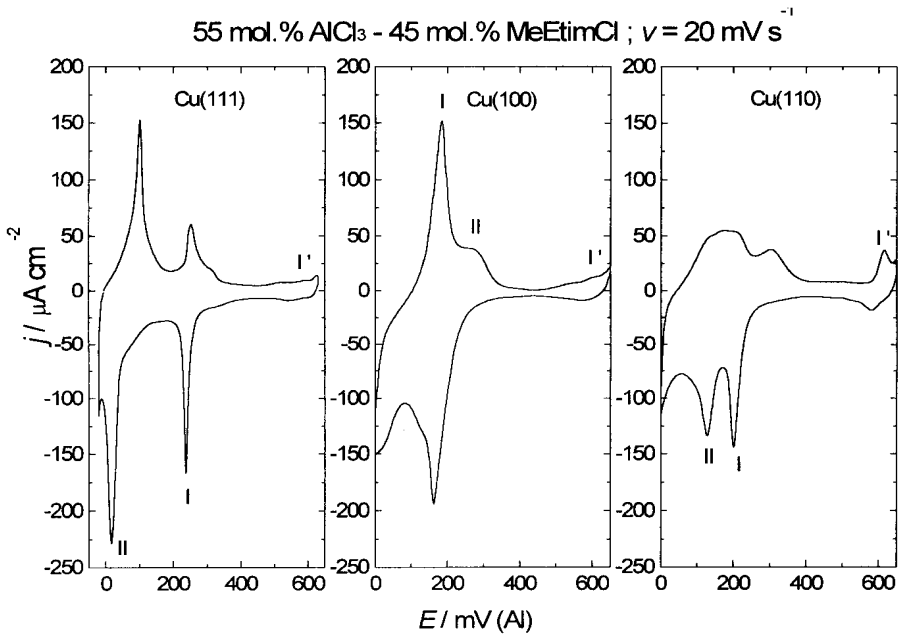

Fig. 4. Cyclic voltammograms of the UPD of Al onto Cu(111), Cu(100) and Cu(110).

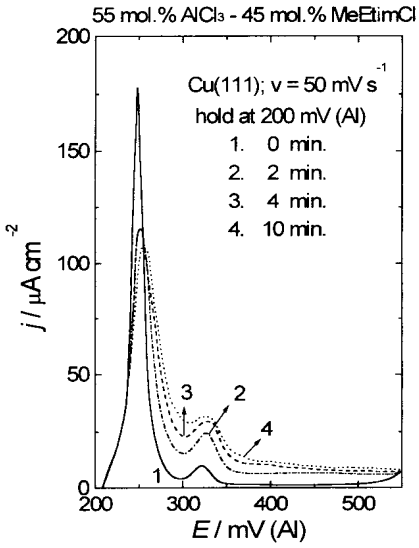

Fig. 5. Anodic voltammograms recorded after holding Cu(111) electrode at the potential of 200 mV vs. Al for different time intervals (0 min to 10 min.).

Cyclic voltammograms recorded onto Cu(111), Cu(100) and Cu(110) are shown in Fig. 4. It can be seen that UPD of Al commences at about 300 mV vs. Al on all three faces (peaks I and II), although a pair of small peaks (I ') appears at more positive potentials, close to the potential of Cu dissolution. These peaks are more pronounced on more open surfaces, such as (100) and (110). The peak current vs. sweep rate dependence for both, anodic and cathodic peaks, is linear, indicating simple adsorption of some species. On all three faces UPD is characterized by two peaks. The sharpest and well separated peaks are obtained on the Cu(111), indicating the formation of two different adsorbed structures. The charge under the peak I corresponds to the coverage of 25%, while the combined charge for peaks I and II is consistent with the deposition of a full monolayer of Al onto Cu.

It is interesting to note that alloying of Cu with Al starts at the potential of peak I, which is not a common feature for UPD systems in aqueous solutions [16]. This phenomenon is clearly indicated in Fig. 5, where the Cu(111) electrode was held at

E = 200 mV vs. Al for different time intervals (0 min. to 10 min.) and corresponding anodic voltammograms were recorded. The charge under the anodic peaks increases with the time of holding and after 10 min. approaches twice that recorded without holding. Hence, alloying of Cu with Al takes place during the UPD process, which explains the fact that the cathodic peaks are better defined than anodic ones. As can be seen in Fig. 4, this phenomenon is more pronounced on the more open surfaces, such as Cu(100) and Cu(110).

REFERENCES

[1] C.L. Hussey, Chemistry of Nonaqueous Solutions: Current Progress, G. Mamantov, A.I. Popov, Editors, pp. 227-275, VCH Publishers, New York (1994).

[2] C.L. Hussey, T.B. Scheffler, J.S. Wilkes, A.A. Fannin, Jr., J. Electrochem. Soc., **133**, 1389 (1986).

[3] T.P. Moffat, J. Electrochem. Soc., **141**, 3059 (1994).

[4] R.J. Gale, B. Gilbert, R.A. Osteryoung, Inorg. Chem., **18**, 2723 (1979).

[5] L. Heerman, W. D'Olieslager, Proc. of the Ninth International Symposium on Molten Salts, PV 94-13, p. 441, The Electrochemical Society, Pennington, NJ (1994).

[6] W.R. Pitner, C.L. Hussey, G.R. Stafford, J. Electrochem. Soc., **143**, 130 (1996).

[7] R.T. Carlin, P.C. Trulove, H.C. De Long, J. Electrochem. Soc., **143**, 2747 (1996).

[8] J.A. Mitchell, W.R. Pitner, C.L. Hussey, G.R. Stafford, J. Electrochem. Soc., **143**, 3448 (1996).

[9] C.L. Hussey, L.A. King, R.A. Carpio, J. Electrochem. Soc., **126**, 1029 (1979).

[10] B.J. Tierney, W.R. Pitner, J.A. Mitchell, C.L. Hussey, G.R. Stafford, J. Electrochem. Soc., **145**, 3110 (1998).

[11] C.L. Hussey, X. Xu, J. Electrochem. Soc., **138**, 1886 (1991).

[12] J.S. Wilkes, J.A. Levisky, R.A. Wilson, C.L. Hussey, Inorg. Chem., **21**, 1263 (1982).

[13] J.L. Murray, Phase Diagrams of Binary Copper Alloys, P.R. Subramanian, D.J. Chakrabarti, D.E. Laughlin, Editors, American Society for Metals, Metals Park, OH (1994).

[14] H. Warlimont, M. Wilkens, Z. Metallk., **55**, 382 (1964).

[15] J. Gala, E. Lagiewka, J. Baranska, J. Appl. Electrochem., **11**, 735 (1981).

[16] D.M. Kolb, Advances in Electrochemistry and Electrochemical Engineering, Vol.11, H. Gerischer, C.W Tobias, Editors, John Wiley, New York (1978).